Linker Functionalization in MIL-47(V)-R Metal–Organic Frameworks:
Understanding the Electronic Structure
Supplementary material

Supporting Information for 'Linker Functionalization of MIL-47(V)-R Metal-Organic Frameworks: Understanding the Electronic Structure'

Danny E. P. Vanpoucke[1, 2, *]

[1] *UHasselt, Institute for Materials Research (IMO-IMOMEC), Agoralaan, 3590 Diepenbeek, Belgium*
[2] *IMOMEC, IMEC vzw, 3590 Diepenbeek, Belgium*

CONTENTS

S1.   COMPUTATIONAL DETAILS

For the series of structures under study we perform *ab-initio* density functional theory (DFT) calculations within the projector augmented wave (PAW) method as implemented in the Vienna *ab-initio* Package (VASP) program using the generalized gradient approximation (GGA) functional as constructed by Perdew, Burke and Ernzerhof (PBE).[1–5] The plane wave kinetic energy cutoff is set to 500 eV. Due to the large difference in lattice vector lengths for the structures a Monkhorst-Pack special k-point grid of $2 \times 2 \times 6$ k-points is used to sample the Brillouin zone.[6,7] Dispersive interactions, which play an important role in the flexibility of the crystal structure of MOFs, are included through the DFT-D method as suggested by Grimme *et al.*, including Becke-Johnson damping.[8–11]. To obtain an accurate picture of the electronic structure, hybrid functional, HSE06+D,[12–14] calculations are performed on the PBE optimized geometries, as this was previously shown to give very accurate estimates of the experimental band gap in MOFs.[15]

The atomistic model used in our DFT calculations consisted of a conventional unit cell containing four formula units (*i.e.* containing 72 to 88 atoms). Figure 1 shows a ball-and-stick representation of the large pore MIL-47(V) structure (a super cell is shown). Starting from the experimental lattice parameters and volumes the structures are optimized under the constraint of constant volume to allow for direct comparison to the experimental results.[7] Ionic positions and cell shape are optimized simultaneously using a conjugate gradient method, and convergence is set to the difference in energy between subsequent steps becoming smaller than 1.0×10^{-7} eV. After full relaxation, the forces on the ions were found to be below 0.002 eV/Å.

As each of the four vanadium atoms (two V atoms on each vanadyl chain in the conventional unit cell) contributes one unpaired electron to the system, and it is known that the configuration of these unpaired spins has a strong influence on the electronic structure and mechanical properties of flexible MOFs,[16] we considered two different spin configurations for each of the structures: the anti-ferromagnetic (AF) ground state configuration[17] and the ferromagnetic (FM) configuration. The presence of both configurations in experimental samples has been derived from X-Ray Diffraction data.[18] The different spin configurations are manually imposed upon initialization of the structure optimization by setting the initial magnetic moment for each atom in the cell (MAGMOM keyword). For each following calculation the atomic magnetic moments are checked, and it is verified that the imposed spin configuration is retained. If this is not the case, the magnetic moment is reinitialized and the structure optimization is continued from this point.

The atomic charges of the systems are calculated using the iterative Hirshfeld-I approach[19] as implemented in our in house developed code HIVE.[20–22] Our implementation makes use of the grid stored (pseudo) electron density distributions which are standardly obtained from VASP.[21,22] The atom centered spherical integrations are done using Lebedev-Laikov grids of 1202 grid points per shell, and a logarithmic radial grid.[23,24] The iterative scheme is considered converged when the largest difference in charge of a system atom is less than 1.0×10^{-5} electron in two consecutive iterations.

The total amount of calculation time for the current work exceeds 33 years CPU(-core)-time (Sandy Bridge, E5-2670, 2.6 GHz).

S2. STRUCTURE INFORMATION

Although the total energy differs significantly between the AF and FM structures, the underlying atomic structure shows only very minute differences. These, however, can still be discerned in very detailed XRD analysis, allowing for direct comparison with experiment.[18] The optimized atomic structures can be obtained free of charge from The Cambridge Crystallographic Data Centre: CCDC 1507811–1507830.

TABLE S1. Structural parameters of functionalized MIL-47(V)-X MOFs with a FM spin configuration. Lattice parameters a, b, and c are given, as well as the volume of a unit cell containing 4 formula units (72–88 atoms). The opening angle of the MOF θ and the linker rotation angle ϕ are defined in Fig. 1.

	a (Å)	b (Å)	c (Å)	Vol (Å^3)	θ (°)	ϕ (°)
MIL-47(V)	16.319	13.918	6.826	1550.344	80.9	8.5
-F	16.436	13.841	6.849	1558.092	80.2	9.2
-Cl	16.987	13.116	6.829	1521.587	75.3	21.8
-Br	16.482	13.760	6.848	1553.001	79.7	24.1
-2,5F	17.795	11.996	6.819	1455.568	68.0	12.6
-OH	16.729	13.428	6.842	1537.046	77.5	3.2
-CH$_3$	16.796	13.324	6.829	1528.355	76.9	20.5
-CF$_3$	16.175	14.111	6.867	1567.271	82.2	30.9
-OCH$_3$	16.944	13.144	6.828	1520.498	75.6	28.6

S3.   ATOMIC CHARGES

TABLE S2. Hirshfeld-I atomic charges [in electron] for the different atoms as indicated in Fig. 1c. For the 2×-F system, the charge of the functional group presented is that of a single -F functional group. The PBE-electron density for the FM systems was.

	V	O_V	O_{BDC}	C_O	R	C_R	C_1	C_2	C_3	C_4	C_5	H_1	H_3	H_4
MIL-47(V)	2.42	−1.01	−0.73	0.78	−	−0.08	−0.08	−0.11	−0.08	−0.08	−0.11	0.12	0.12	0.12
-F	2.42	−1.00	−0.73	0.79	−0.13	0.36	−0.25	−0.07	−0.11	−0.04	−0.26	0.15	0.12	0.12
-Cl	2.42	−1.01	−0.73	0.79	0.04	0.14	−0.25	−0.07	−0.11	−0.04	−0.26	0.15	0.12	0.12
-Br	2.42	−1.01	−0.73	0.79	0.08	0.09	−0.16	−0.09	−0.10	−0.07	−0.17	0.13	0.12	0.11
-2,5F	2.42	−1.00	−0.73	0.81	−0.13	0.34	−0.22	−0.22	−	−	−	0.16	−	−
-OH	2.42	−1.01	−0.73	0.80	−0.10	0.39	−0.23	−0.08	−0.12	−0.03	−0.30	0.14	0.12	0.12
-CH$_3$	2.42	−1.01	−0.73	0.79	−0.05	0.20	−0.15	−0.10	−0.10	−0.07	−0.18	0.12	0.12	0.12
-CF$_3$	2.42	−1.00	−0.73	0.78	0.12	−0.18	−0.08	−0.10	−0.07	−0.08	−0.08	0.12	0.13	0.12
-OCH$_3$	2.42	−1.00	−0.73	0.79	0.04	0.32	−0.26	−0.07	−0.13	−0.06	−0.25	0.13	0.12	0.13

TABLE S3. Hirshfeld-I atomic charges [in electron] for the different atoms as indicated in Fig. 1c. For the 2×-F system, the charge of the functional group presented is that of a single -F functional group. The HSE06-electron density for the AF systems was used, and PBE reference density for reference atomic densities used to construct the promolecule/solid in the Atoms-In-Molecules scheme.

|	V	O_V	O_{BDC}	C_O	R	C_R	C_1	C_2	C_3	C_4	C_5	H_1	H_3	H_4
MIL-47(V)	2.59	−1.08	−0.80	0.89	−	−0.08	−0.08	−0.14	−0.08	−0.08	−0.14	0.12	0.12	0.12
-F	2.59	−1.07	−0.80	0.90	−0.16	0.40	−0.26	−0.08	−0.11	−0.04	−0.29	0.16	0.13	0.13
-Cl	2.59	−1.07	−0.81	0.90	0.03	0.16	−0.18	−0.10	−0.10	−0.06	−0.22	0.14	0.13	0.12
-Br	2.59	−1.07	−0.81	0.90	0.06	0.12	−0.16	−0.11	−0.09	−0.06	−0.20	0.14	0.13	0.12
-2,5F	2.59	−1.07	−0.80	0.91	−0.16	0.38	−0.22	−0.24	−	−	−	0.16	−	−
-OH	2.59	−1.07	−0.81	0.91	−0.12	0.43	−0.24	−0.09	−0.13	−0.02	−0.34	0.15	0.13	0.13
-CH$_3$	2.59	−1.07	−0.80	0.89	−0.05	0.21	−0.15	−0.12	−0.10	−0.07	−0.20	0.13	0.13	0.12
-CF$_3$	2.59	−1.07	−0.80	0.89	0.12	−0.19	−0.07	−0.12	−0.06	−0.08	−0.09	0.13	0.14	0.13
-OCH$_3$	2.59	−1.07	−0.80	0.90	0.06	0.36	−0.27	−0.08	−0.13	−0.05	−0.28	0.14	0.13	0.13

S4

S4. ELECTRONIC STRUCTURE
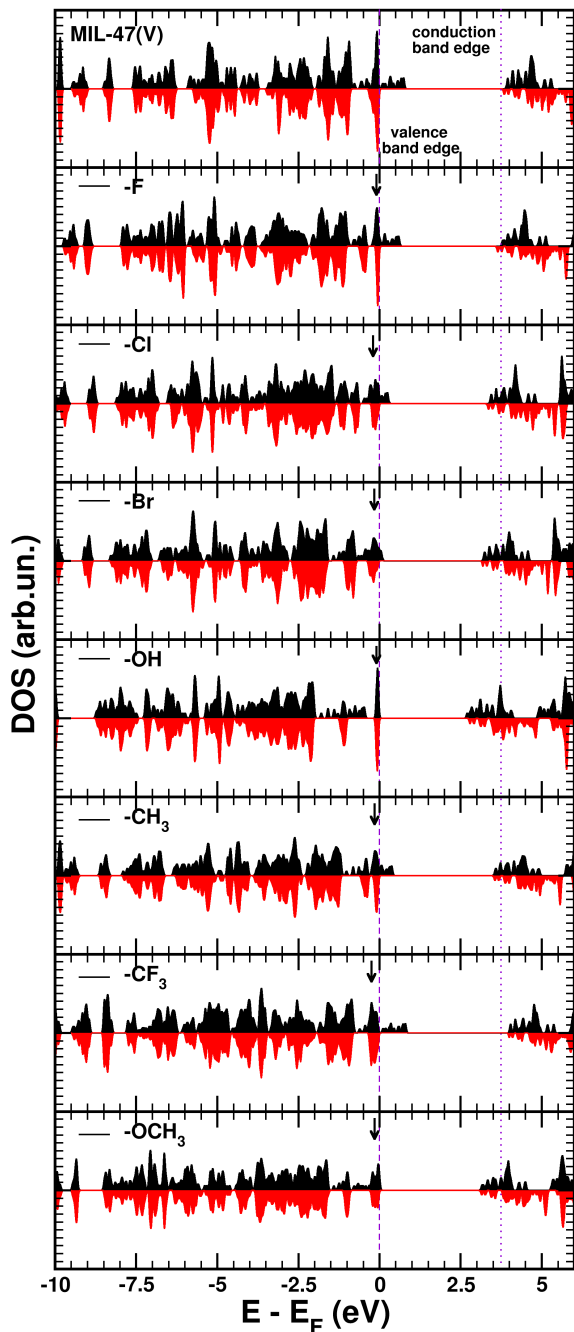
FIG. S1. The total DOS of the MIL-47(V) and the functionalized MOFs, obtained for the HSE06 hybrid functional and the FM spin configuration. The valence and conduction band edges of the unfunctionalized MIL-47(V) AF system are indicated by the dashed and dotted lines, respectively. The position of the split-off π-band is indicated by the arrows. Majority and minority spin components are shown in black and red, respectively. The DOS was smoothed using a 25 meV wide gaussian smoothing function.
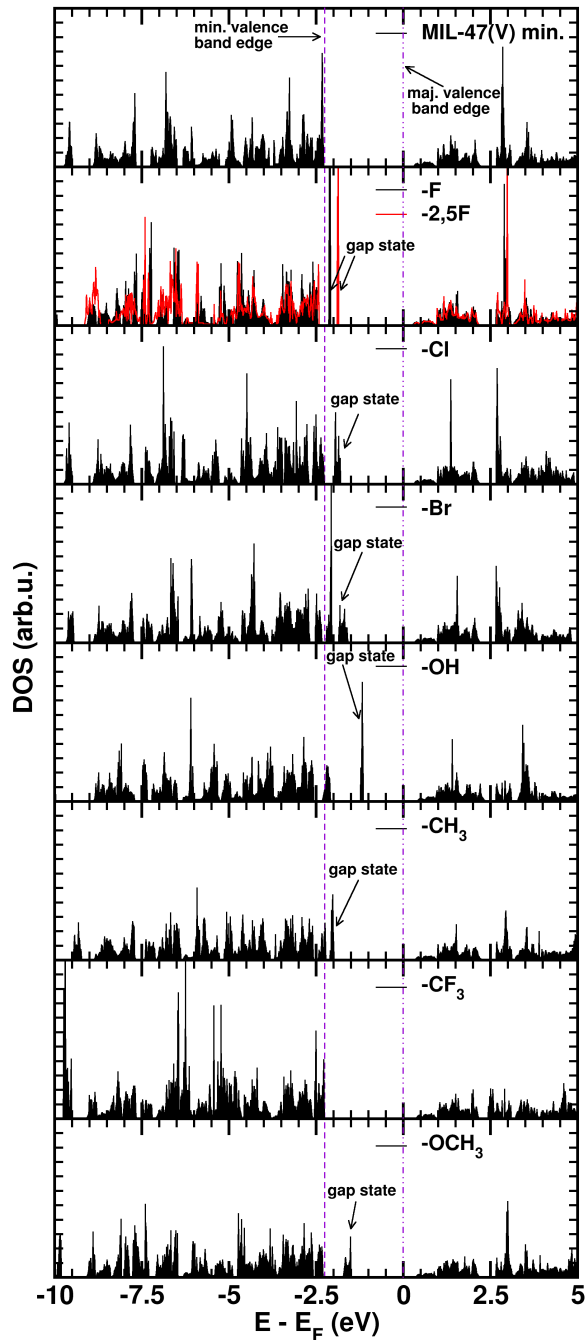
FIG. S2. Total DOS for the minority spin component for the functionalized MIL-47(V) MOFs with a FM spin configuration using the PBE functional. The unfunctionalized MIL-47(V) (top panel) is provided as reference. The top of the minority (dashed line) and majority (dashed-dotted line) spin components of the unfunctionalized MIL-47(V) are indicated. The position of the split-off π-band induced by the functionalization is indicated as "gap state(s)", since it is located in the minority band gap. The functional group is noted in each panel.
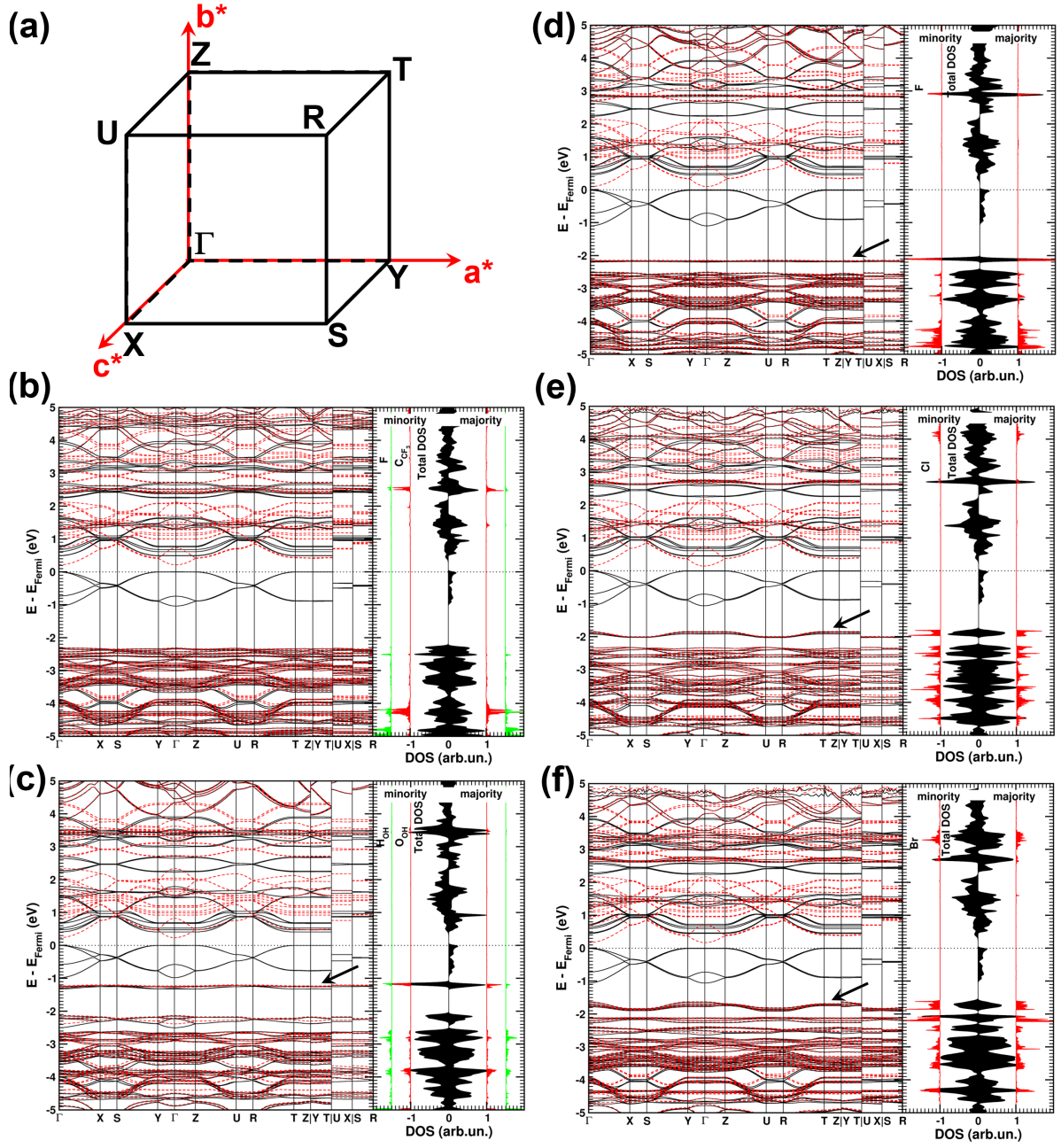
FIG. S3. Electronic band structure (left) and DOS(right) for selected functionalizations. Calculations were performed using the PBE functional for the FM spin configuration of the unpaired vanadium d-electrons. Majority and minority spin bands are given by solid black lines and red dashed lines respectively. In addition to the total DOS, also the atom-projected DOS is given for the atoms of the functional group. The split-off π-bands are indicated with an arrow.
(a) First Brillouin zone with high symmetry points indicated. (b) MIL-47(V)-CF$_3$, (c) MIL-47(V)-OH, (d) MIL-47(V)-F, (e) MIL-47(V)-Cl and, (f) MIL-47(V)-Br
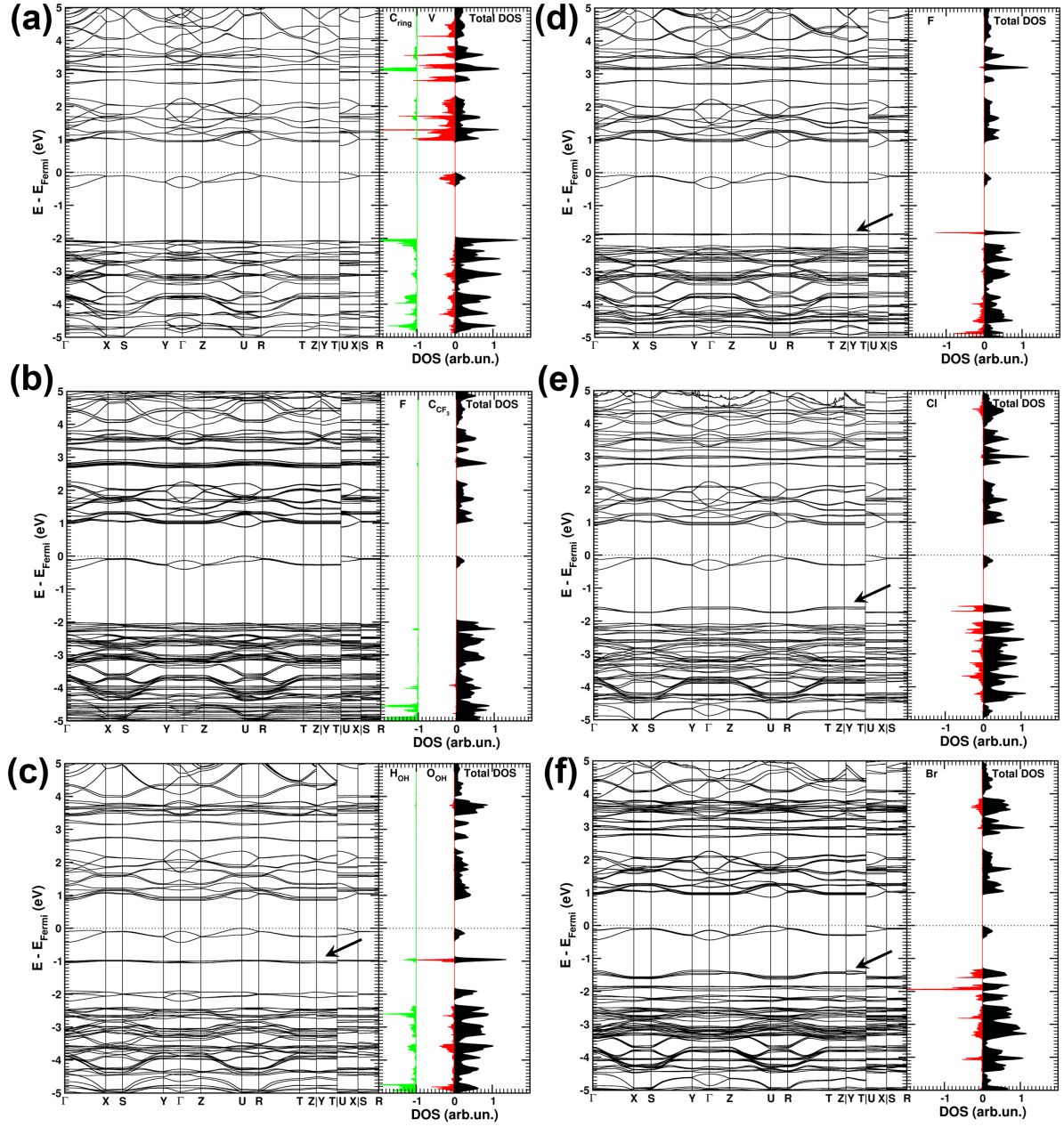
FIG. S4. Electronic band structure (left) and DOS(right) for selected functionalizations. Calculations were performed using the PBE functional for the AF spin configuration of the unpaired vanadium d-electrons. Majority and minority spin bands are exactly the same. In addition to the total DOS, also the atom-projected DOS(flipped to the negative side of the scale) is given for the atoms of the functional group. The split-off π-bands are indicated with an arrow.
(a) Unfunctionalized MIL-47(V). (b) MIL-47(V)-CF$_3$, (c) MIL-47(V)-OH, (d) MIL-47(V)-F, (e) MIL-47(V)-Cl and, (f) MIL-47(V)-Br

REFERENCES

[*] corresponding author: Danny.Vanpoucke@UHasselt.be

[1] P. E. Blöchl, Phys. Rev. B **50**, 17953 (1994).

[2] G. Kresse and D. Joubert, Phys. Rev. B **59**, 1758 (1999).

[3] J. P. Perdew, K. Burke, and M. Ernzerhof, Phys. Rev. Lett. **77**, 3865 (1996).

[4] G. Kresse and J. Hafner, Phys. Rev. B **47**, 558 (1993).

[5] G. Kresse and J. Furthmüller, Phys. Rev. B **54**, 11169 (1996).

[6] H. J. Monkhorst and J. D. Pack, Phys. Rev. B **13**, 5188 (1976).

[7] D. E. P. Vanpoucke, K. Lejaeghere, V. V. Speybroeck, M. Waroquier, and A. Ghysels, J. Phys. Chem. C **119**, 23752 (2015).

[8] A. M. Walker, B. Civalleri, B. Slater, C. Mellot-Draznieks, F. Cor, C. M. Zicovich-Wilson, G. Romn-Prez, J. M. Soler, and J. D. Gale, Angew. Chem. Int. Ed. **49**, 7501 (2010).

[9] S. Grimme, J. Comput. Chem. **27**, 1787 (2006).

[10] S. Grimme, J. Antony, S. Ehrlich, and H. Krieg, J. Chem. Phys. **132**, 154104 (2010).

[11] S. Grimme, S. Ehrlich, and L. Goerigk, J. Comput. Chem. **32**, 1456 (2011).

[12] J. Heyd, G. E. Scuseria, and M. Ernzerhof, The Journal of Chemical Physics **118**, 8207 (2003).

[13] J. Heyd, J. E. Peralta, G. E. Scuseria, and R. L. Martin, The Journal of Chemical Physics **123**, 174101 (2005).

[14] J. Moellmann and S. Grimme, J. Phys. Chem. C **118**, 7615 (2014).

[15] K. Hendrickx, D. E. P. Vanpoucke, K. Leus, K. Lejaeghere, A. V. Y.-D. Deyne, V. V. Speybroeck, P. V. D. Voort, and K. Hemelsoet, Inorg. Chem. **54**, 10701 (2015).

[16] D. E. P. Vanpoucke, J. W. Jaeken, S. D. Baerdemacker, K. Lejaeghere, and V. V. Speybroeck, Beilstein J. Nanotechnol. **5**, 1738 (2014).

[17] K. Barthelet, J. Marrot, D. Riou, and G. Férey, Angew. Chem. Int. Ed. **41**, 281 (2002).

[18] T. Bogaerts, L. Vanduyfhuys, D. E. P. Vanpoucke, J. Wieme, M. Waroquier, P. Van Der Voort, and V. Van Speybroeck, CrystEngComm **17**, 8612 (2015).

[19] P. Bultinck, C. Van Alsenoy, P. W. Ayers, and R. Carbó-Dorca, J. Chem. Phys. **126**, 144111 (2007).

[20] D. E. P. Vanpoucke, "HIVE v3.x," `http://dannyvanpoucke.be/` (2009–2017).

[21] D. E. P. Vanpoucke, P. Bultinck, and I. Van Driessche, J. Comput. Chem. **34**, 405 (2013).

[22] D. E. P. Vanpoucke, I. Van Driessche, and P. Bultinck, J. Comput. Chem. **34**, 422 (2013).

[23] A. D. Becke, J. Chem. Phys. **88**, 2547 (1988).

[24] V. I. Lebedev and D. Laikov, Doklady Mathematics **59**, 477 (1999).